

# Improving Signed Propagation of Graph Neural Network Under Multiple Classes

Yoonhyuk Choi<sup>1</sup>, Jiho Choi<sup>2</sup>, Taewook Ko<sup>3</sup>, Chong-Kwon Kim<sup>4</sup>

Arizona State University (Tempe)<sup>1</sup>, KAIST<sup>2</sup>, Seoul National Univesrity<sup>3</sup>, Korea Institute of Energy Technology<sup>4</sup>

Computer Engineering<sup>1,2,3</sup>, Energy AI<sup>4</sup>

United States<sup>1</sup>, South Korea<sup>2,3,4</sup>

{chldbsgur123,jihochoi1993,taewook.ko}@gmail.com, ckim@kentech.ac.kr

**Abstract**—Graph Neural Networks (GNNs) exhibit satisfactory performance on homophilic networks, where most edges connect two nodes with the same label. However, their effectiveness diminishes as the graphs become heterophilic (low homophily), prompting the exploration of various message-passing schemes. In particular, assigning negative weights to heterophilic edges (signed propagation) for message-passing has gained significant attention, and some studies theoretically confirm its effectiveness. Nevertheless, prior theorems assume binary classification scenarios, which may not hold well for graphs with multiple classes. To solve this limitation, we offer new theoretical insights into GNNs in multi-class environments and identify the drawbacks of employing signed propagation from two perspectives: message-passing and parameter update. We found that signed propagation without considering feature distribution can degrade the separability of dissimilar neighbors, which also increases prediction uncertainty (e.g., conflicting evidence) that can cause instability. To address these limitations, we introduce two novel calibration strategies aiming to improve discrimination power while reducing entropy in predictions. Through theoretical and extensive experimental analysis, we demonstrate that the proposed schemes enhance the performance of both signed and general message-passing neural networks.

**Index Terms**—Graph neural network, semi-supervised learning, graph heterophily, signed propagation, multi-class dataset

## I. INTRODUCTION

The recent proliferation of graph-structured datasets has ignited rapid advancements in graph mining techniques. Especially, Graph Neural Networks (GNNs) provide satisfactory performances in various downstream tasks including node classification and link prediction. The main component of GNNs is message-passing [1], where information is propagated between adjacent nodes and aggregated. Additionally, the entailment of a structural property enhances the representation and the discrimination powers of GNNs [2, 3].

Early GNNs assume the network homophily, where nodes of similar features make connections based on social influence and/or selection theories. Spectral GNNs [1, 2] employ Laplacian smoothing called low-pass filtering to receive low-frequency signals from neighbor nodes. Consequently, these methods fail to adequately address heterophilous graphs [4] and show dismal performance [5] in several heterophilous cases. To resolve this problem, numerous clever algorithms (spatial GNNs) have been proposed, including adjustment of edge coefficients [3, 6] and aggregation of remote but

highly similar nodes [7, 8]. However, most of these methods assume positive or unsigned edges, which may impoverish the separation power [9].

Recently, several studies [10, 11] have applied message passing over negative (signed propagation) edges to preserve high-frequency signal exchanges. From the viewpoint of gradient flow, [12] shows that negative eigenvalues can intensify high-frequency signals during propagation. On the other hand, [13] prevents message diffusion by assigning zero-weights (blocking information) to heterophilic edges to alleviate local smoothing. Based on this observation, we raise a question: *does signed propagation always attain the best performance on heterophilic graphs?*

To address the above question, we focus on the recent investigations [5, 9] that provide valuable insights on message-passing. These studies mathematically analyze the effect of unsigned and signed messages on separability by comparing node feature distributions before and after message passing and aggregation. Furthermore, they reveal that signed messaging always enhances performance on heterophilic graphs. However, our empirical analysis (Fig. 3) shows that this assertion may not hold well under real-world graphs. This discrepancy arises because the prior work assumes binary class graphs [14], impeding their extension to multi-class graphs.

In this paper, we deal with signed messaging on multi-class graphs. We first demonstrate that blind application of signed messaging to multi-class graphs may incur significant performance degradation. To overcome the problem, we propose to utilize two types of calibration [15, 16], which are simple yet effective in enhancing the performance of signed GNNs. In summary, our contributions can be described as follows:

- Contrary to the prior work confined to binary class graphs, we address the issues when the signed messaging mechanism is extended to a multi-class scenario. Our work provides fundamental insight into using signed messages and establishes the theoretical background for developing powerful GNNs.
- We hypothesize and prove that signed propagation may reduce the discrimination power in certain cases while increasing prediction uncertainties. Expanding this understanding, we propose novel strategies based on two types of calibration that are shown to be effective for both signed and unsigned GNNs.

- We perform extensive experiments with real-world benchmark datasets to validate our theorems. Our experiments demonstrate the effectiveness of the proposed calibration techniques.

## II. RELATED WORK

**Graph Neural Networks (GNNs).** Aggregating the information from adjacent nodes, GNNs have shown great potential under semi-supervised learning settings. Early study [1] focused on the spectral graph analysis (e.g., Laplacian decomposition) in a Fourier domain. However, it suffers from large computational costs as the graph scale increases. GCN [2] reduced the overhead by harnessing the localized spectral convolution through the first-order approximation of a Chebyshev polynomial. Another notable approach is spatial-based GNNs [3, 6, 17, 18] which aggregate information in a Euclidean domain. Early spatial techniques have led to the development of many powerful schemes that encompass remote nodes as neighbors.

**GNNs on Heterophilic Graphs.** Traditional message-passing GNNs fail to perform well in heterophilic graphs [7]. To redeem this problem, recent studies have focused on handling disassortative edges [19–22] by capturing node differences or by incorporating similar remote nodes as neighbors. More recently, H<sub>2</sub>GCN [4] suggests the separation of ego and neighbors during aggregation. As another branch, selecting neighbors from non-adjacent nodes [8], configuring path-level pattern [23], finding a compatibility matrix [24], employing adaptive propagation [25], and choosing appropriate architectures [26] have been recently proposed. Some methodologies change the sign of disassortative edges from positive to negative [10, 11, 27, 28] while others assign zero-weights to disassortative edges [13]. Even though [29] demonstrates that signed propagation can effectively handle binary class graphs, further investigation may be needed before applying the same techniques to multi-class graphs.

## III. PRELIMINARY

Let  $\mathcal{G} = (\mathcal{V}, \mathcal{E}, X)$  be a graph with  $|\mathcal{V}| = n$  nodes and  $|\mathcal{E}| = m$  edges. The node attribute matrix is  $X \in \mathbb{R}^{n \times F}$ , where  $F$  is the dimension of an input vector. Given  $X$ , the hidden representation of node features  $H^{(l)}$  at the  $l$ -th layer is derived through message-passing. Here, node  $i$ 's feature is defined as  $h_i^{(l)}$ . The structural property of  $\mathcal{G}$  is represented by its adjacency matrix  $A \in \{0, 1\}^{n \times n}$ . A diagonal matrix  $D$  of node degrees is derived from  $A$  as  $d_{ii} = \sum_{j=1}^n A_{ij}$ . Each node has its label  $Y \in \mathbb{R}^{n \times C}$  ( $C$  represents the number of classes). Lastly, the global edge homophily ratio,  $\mathcal{H}_g$ , is defined as:

$$\mathcal{H}_g \equiv \frac{\sum_{(i,j) \in \mathcal{E}} \mathbb{1}(Y_i = Y_j)}{|\mathcal{E}|} \quad (1)$$

Likewise, the local homophily ratio,  $b_i$ , of node  $i$  is given as:

$$b_i \equiv \frac{\sum_{j=1}^n A_{ij} \cdot \mathbb{1}(Y_i = Y_j)}{d_{ii}} \quad (2)$$

Given a partially labeled training set  $\mathcal{V}_L$ , the goal of semi-supervised node classification is to correctly predict the classes of unlabeled nodes  $\mathcal{V}_U = \{\mathcal{V} - \mathcal{V}_L\} \subset \mathcal{V}$ .

## IV. THEORETICAL ANALYSIS

We first discuss the mechanism of GNNs in terms of message-passing and parameter update (§IV-A). Then, we introduce previous analyses of signed message passing on binary class graphs (§IV-B) and highlight some misunderstandings revealed through an empirical study with real-world datasets (§IV-C). Based on this observation, we extend the prior analysis to a multi-class scenario and point out some drawbacks of signed messaging in more complicated environments (§IV-D).

### A. Message-Passing Neural Networks

Generally, GNNs employ alternate steps of propagation and aggregation recursively, during which the node features are updated iteratively. This is widely known as message-passing, which can be represented as follows:

$$H^{(l+1)} = \phi(\bar{H}^{(l+1)}), \quad \bar{H}^{(l+1)} = AH^{(l)}W^{(l)} \quad (3)$$

Here,  $H^{(0)} = X$  is the initial vector and  $H^{(l)}$  is nodes' hidden representations at the  $l$ -th layer.  $\bar{H}^{(l+1)}$  is retrieved through message-passing ( $A$ ) and we obtain  $H^{(l+1)}$  after an activation function  $\phi$ .  $W^{(l)}$  is trainable weight matrices shared by all nodes. The final prediction is produced by applying cross-entropy  $\sigma(\cdot)$  (e.g., log-softmax) to  $\bar{H}^{(L)}$  and the loss function is defined as below:

$$\mathcal{L}_{GNN} = \mathcal{L}_{nll}(Y, \hat{Y}), \quad \hat{Y} = \sigma(\bar{H}^{(L)}) \quad (4)$$

The parameters are updated by computing negative log-likelihood loss  $\mathcal{L}_{nll}$  between the predictions ( $\hat{Y}$ ) and true labels ( $Y$ ). Since most GNNs assume homophily, they tend to preserve the low-frequency information (local smoothing) [30]. As a result, they fail to pinpoint the differences between heterophilic neighbors and show dismal performance [7, 31]. Recent studies [9–11, 32] focus on the extraction of high-frequency signals by flipping the sign of disassortative edges from positive to negative. In the following sections, we analyze the influence of information propagation from the perspectives of **message-passing** (Eq. 3) and **parameter update** (Eq. 4).

### B. Using Signed Messages on Binary Classes

Before delving into the multi-class graphs, we assess the implications of signed propagation with graphs containing only two types of classes [9, 29].

**Message-passing** (*Signed propagation always has a better discrimination power than all positive propagation*) For brevity, we take GCN [2] as an example to inspect how message passing alters node feature vectors. Assuming a binary label ( $y_i \in \{0, 1\}$ ), let us inherit several assumptions and notations from [9] as follows: (1) For all nodes  $i = \{1, \dots, n\}$ , their degrees  $\{d_i\}$  and features  $\{h_i\}$  are *i.i.d.* random variables. (2) Every class has the same population. (3) With a slight abuse of notation, assume that  $h^{(0)} = XW^{(0)}$  is

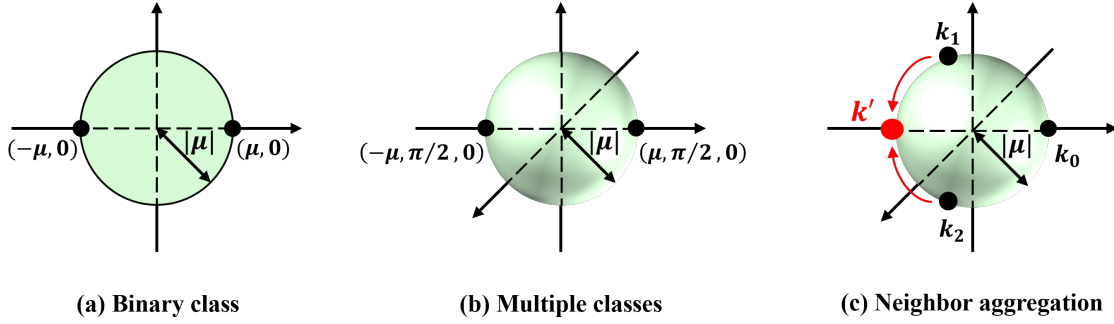


Fig. 1: We take an example to illustrate the distribution of node features under (a) binary and (b) multi-class scenarios. Figure (c) represents the aggregation of neighboring nodes ( $k_1, k_2$ ) under multiple classes, where the scale of aggregated vector  $k'$  is always smaller than  $|\mu|$

the first layer projection of the initial node features. (4) The node feature of label  $y_i$  follows the distribution ( $\mu$  or  $-\mu$ ) as,

$$\mathbb{E}(h_i^{(0)}|y_i) = \begin{cases} \mu, & \text{if } y_i = 0 \\ -\mu, & \text{if } y_i = 1 \end{cases} \quad (5)$$

We first introduce the equations from prior work [9] (Eq. 7 and Eq. 8), which demonstrate the updates in the expectations of node  $i$ 's latent features  $\mathbb{E}(h_i^{(0)}|y_i)$  after a single-hop application of message passing  $\mathbb{E}(h_i^{(1)}|y_i, d_i)$  below:

$$h_i^{(1)} = \frac{h_i^{(0)}}{d_i + 1} + \sum_{j \in \mathcal{N}_i} \frac{h_j^{(0)}}{\sqrt{(d_i + 1)(d_j + 1)}} \quad (6)$$

**(Vanilla GCN)** As illustrated in Figure 1a (binary class), we assume  $h_i \sim N(\mu, 0)$  for  $y_i = 0$ . Otherwise,  $h_i \sim N(-\mu, 0)$ . Let us assume that  $1/d_{ij} = 1/\sqrt{(d_i + 1)(d_j + 1)}$ . Then, the updated node feature  $\mathbb{E}(h_i^{(1)}|v_i, d_i)$  derived through the message-passing of vanilla GCN (Eq. 6) is as follows:

$$\begin{aligned} \mathbb{E}(h_i^{(1)}|v_i, d_i) &= \frac{\mu}{d_i + 1} + \sum_{j \in \mathcal{N}_i} \left( \frac{b_j}{d_{ij}} \mu - \frac{(1 - b_j)}{d_{ij}} \mu \right) \\ &= \left( \frac{1}{d_i + 1} + \frac{2b_i - 1}{d_i + 1} \sum_{j \in \mathcal{N}_i} \frac{\sqrt{d_i + 1}}{\sqrt{d_j + 1}} \right) \mu \\ &= \left( \frac{1 + (2b_i - 1)d'_i}{d_i + 1} \right) \mu \quad * d'_i = \sum_{j \in \mathcal{N}_i} \frac{1}{d_{ij}} \end{aligned} \quad (7)$$

**(Signed GCN)** To define the mechanism of signed GCN, we need to assume an error ratio  $e$  that stands for the accuracy ( $1 - e$ ) of configuring the sign of heterophilous edges. Considering that the sign of heterophilous nodes is flipped inaccurately with a probability  $e$ , the update of the signed GCN can be

defined as below:

$$\begin{aligned} \mathbb{E}(h_i^{(1)}|v_i, d_i) &= \frac{\mu}{d_i + 1} + \\ &\sum_{j \in \mathcal{N}_i} \left( \frac{\mu(1 - e) - \mu e}{d_{ij}} b_j + \frac{\mu(1 - e) - \mu e}{d_{ij}} (1 - b_j) \right) \\ &= \left( \frac{1}{d_i + 1} + \frac{1 - 2e}{d_i + 1} \sum_{j \in \mathcal{N}_i} \frac{1}{d_{ij}} \right) \mu \\ &= \left( \frac{1 + (1 - 2e)d'_i}{d_i + 1} \right) \mu \end{aligned} \quad (8)$$

Now, we first introduce the expectation changes of zero-weight GCN (blocking message), similar to the ones discussed above.

**Theorem 4.1** (Zero-weight GCN). *Given an error ratio  $e$ , assigning zero weights to heterophilic edges leads to the following update in the expectation of feature distribution:*

$$\begin{aligned} \mathbb{E}(h_i^{(1)}|v_i, d_i) &= \frac{\mu}{d_i + 1} + \sum_{j \in \mathcal{N}_i} \left( \frac{\mu(1 - e)}{d_{ij}} b_j - \frac{\mu e}{d_{ij}} (1 - b_j) \right) \\ &= \left( \frac{1 + (b_i - e)d'_i}{d_i + 1} \right) \mu. \end{aligned} \quad (9)$$

For all message-passing schemes, if the coefficient of  $\mathbb{E}(h_i^{(0)}|y_i)$  is smaller than 1, node feature vectors move towards the decision boundary and message-passing loses its discrimination power [9]. Based on this, we compare the separability of signed GCN and zero-weight GCN below.

**Corollary 4.2** (Comparison of discrimination powers of signed GCN and zero-weight GCN). *Omitting the overlapping part of Eq. 8 and Eq. 9, their difference  $Z$  can be derived using the error ratio and the local homophily ratio as,*

$$Z = (1 - 2e) - (b_i - e) = 1 - e - b_i, \quad (10)$$

where  $0 \leq e, b_i \leq 1$ .

In Figure 2a, we visualize the value  $Z$  in Eq. 10. Note that the space is half-divided because  $\mathbb{E}[Z] = \int_0^1 \int_0^1 (1 - e - b_i) de db_i = 0$ . Since  $Z$  is likely to be positive when  $e$  is small, it suggests that signed GCN outperforms zero-weight

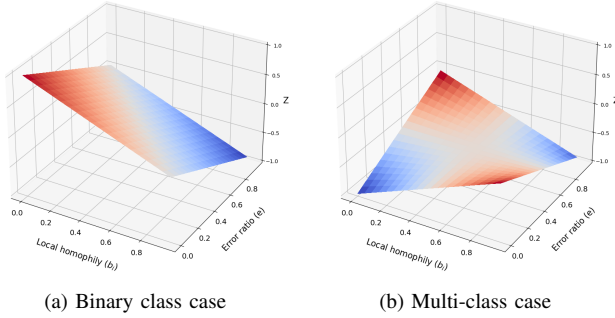


Fig. 2: We plot the  $Z$  in (a) Eq. 10 and (b) Eq. 18 to compare the discrimination powers of signed GCN and zero-weight GCNs. The red and blue colored parts indicate the regions where signed GCN and zero-weight GCN produce superior performances, respectively

GCN. Likewise, we can induce the separability gap of plain (Eq. 7) and signed messaging (Eq. 8) as  $Z = 2(b_i + e - 1)$ , which is likely to be negative when the error ratio is small. Therefore, the equation suggests the superiority of signed GCN over vanilla GCN. To summarize, the above analyses attest that signed messaging might be a good choice for binary graphs.

**Parameter update** (The feature vectors of two nodes connected with a negative edge are separated farther during training) Let us assume that an ego ( $i$ ) and one of its neighbor nodes ( $j$ ) are connected with a negative edge. Please ignore other neighbors to concentrate on the separation effect (sign) of propagated messages. The ego node  $i$ 's feature vector is updated after message-passing as below:

$$\hat{Y}_i = \sigma(\bar{H}_i^L) = \sigma\left(\frac{\bar{H}_i^L}{d_i + 1} - \frac{\bar{H}_j^L}{\sqrt{(d_i + 1)(d_j + 1)}}\right) \quad (11)$$

Given that  $Y_i = k$ , the loss ( $\mathcal{L}_{nl}$ ) between the true label ( $Y_i \in \mathcal{R}^C$ ) and a prediction ( $\hat{Y}_i \in \mathcal{R}^C$ ) is defined as below:

$$\mathcal{L}_{nl}(Y_i, \hat{Y}_i) = -\log(\hat{y}_{i,k}) \quad (12)$$

Accordingly, the update procedure is given as  $\hat{y}_{i,k}^{(t+1)} = \hat{y}_{i,k}^t - \eta \nabla_i \mathcal{L}_{nl}(Y_i, \hat{Y}_i)$  and  $\hat{y}_{j,k}^{(t+1)} = \hat{y}_{j,k}^t - \eta \nabla_j \mathcal{L}_{nl}(Y_i, \hat{Y}_i)$ . Here,  $\eta$  is the learning rate and  $\nabla$  represents a partial derivative. The gradient of node  $j$ ,  $\nabla_j \mathcal{L}_{nl}(Y_i, \hat{Y}_i)_k$ , is given by:

$$\begin{aligned} \nabla_j \mathcal{L}_{nl}(Y_i, \hat{Y}_i)_k &= \frac{\partial \mathcal{L}_{nl}(Y_i, \hat{Y}_i)_k}{\partial \hat{y}_{i,k}} = \frac{\partial \mathcal{L}_{nl}(Y_i, \hat{Y}_i)_k}{\partial \hat{y}_{i,k}} \cdot \frac{\partial \hat{y}_{i,k}}{\partial h_{j,k}^{(L)}} \\ &= -\frac{1}{\hat{y}_{i,k}} \cdot (\hat{y}_{i,k}(1 - \hat{y}_{i,k})(-1)) = 1 - \hat{y}_{i,k} > 0 \end{aligned} \quad (13)$$

Since the column-wise components of the last weight matrix  $W^{(L)}$  (Eq. 3) act as independent classifiers, we can infer that as the training epoch ( $t$ ) progresses, the probability of class  $k$  for node  $j$  ( $\hat{y}_{j,k}$ ) decreases since  $-\eta \nabla_j \mathcal{L}_{nl}(Y_i, \hat{Y}_i) < 0$ .

### C. Empirical Analysis

Through Corollary 4.2 and Eq. 13, we prove that signed propagation is generally advantageous when it is applied to binary class graphs. Now, we examine whether this finding

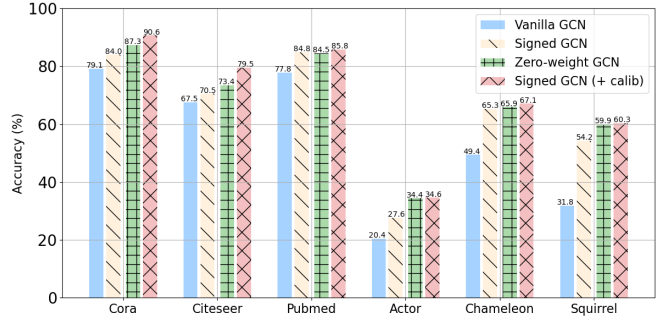


Fig. 3: Node classification accuracy on six benchmark datasets. Vanilla GCN utilizes the original graph, while the coefficient of heterophilous edges is changed to -1 in signed GCN and to 0 in zero-weight GCN, respectively. Here, signed GCN (+ calib) further employs two types of calibration, which is introduced in Section V

is valid on multi-class graphs with more than two classes. In Figure 3, we measure the node classification accuracy of GCN [2] on nine benchmark graphs (the statistical details of the datasets are shown in Table II). Starting from the original GCN called vanilla GCN, we construct two variants; one variant replaces heterophilic edges with -1 (called signed GCN), and the other assigns weight 0 to heterophilic edges (called zero-weight GCN). Since we identified all heterophilous edges, the error ratio is zero. In this case,  $Z (= 1 - b_i)$  derived in Corollary 4.2 has a non-negative value regardless of the local homophily ratio  $b_i$ , meaning that signed GCN outperforms zero-weight GCN. However, Figure 3 shows that zero-weight GCN generally outperforms signed GCN ( $Z \leq 0$ ). To investigate this phenomenon, we extend the theorems to a multi-class scenario and introduce two types of calibration below.

### D. Signed Messaging on Multi-Class Graphs

Through empirical studies, we have confirmed that prior theories do not hold well in multi-class benchmark graphs. We analyze the functioning of signed message propagation on multi-class graphs and uncover several drawbacks from the perspectives of message-passing and parameter updates.

**Message-passing** (Signed propagation may cause impairments in the discrimination power of message-passing) Let us consider a graph with three classes. Without loss of generality, we can extend the same assumptions applied in the binary class case (Eq. 5) to the ternary class case by employing the spherical coordinate as follows:

$$\mathbb{E}(h_i^{(0)} | y_i) = (\mu, \phi, \theta), \quad (14)$$

where  $\mu$  represents the scale of a vector. The direction is determined by two angles  $\phi$  and  $\theta$ . As shown in Figure 1b, this equation satisfies the origin symmetry as in the binary case since  $(\mu, \pi/2, 0) = (-\mu, \pi/2, 0)$ . Based on this, we introduce a novel understanding by extending Eq. 7 and Eq. 8 as follows:

**Theorem 4.3** (Signed GCN). *Let us assume  $y_i = 0$ . For simplicity, we fix the coordinates of the ego  $(\mu, \pi/2, 0)$  as  $k$ , and denote the aggregated neighbors as  $k' = (\mu', \phi', \theta')$ ,*

where  $0 \leq \mu' \leq \mu$ ,  $\phi' = \pi/2$ , and  $0 \leq \theta' \leq 2\pi$  (please see Figure 1c). Then, the expectation of  $h_i^{(1)}$  is defined to be:

$$\begin{aligned} \mathbb{E}(h_i^{(1)}|v_i, d_i) &= \frac{k}{d_i + 1} + \\ &\sum_{j \in \mathcal{N}_i} \left( \frac{k(1-e) - ke b_i}{d_{ij}} + \frac{-k'(1-e) + k'e}{d_{ij}} (1-b_i) \right) \\ &= \frac{(1-2e)\{b_i k + (b_i - 1)k'\}d'_i + k}{d_i + 1} \end{aligned} \quad (15)$$

Assuming the scale of all vectors as  $\mu$ , the aggregated vector  $k'$  always satisfies  $|k'| \leq \mu$  considering the degree-normalization and homophily coefficient ( $1 - b_i \leq 1$ ).

**Theorem 4.4** (Zero-weight GCN). *Likewise, the  $h_i^{(1)}$  driven by zero-weight GCN is:*

$$\begin{aligned} \mathbb{E}(h_i^{(1)}|v_i, d_i) &= \frac{k}{d_i + 1} + \sum_{j \in \mathcal{N}_i} \left( \frac{k(1-e)}{d_{ij}} b_i + \frac{k'e}{d_{ij}} (1-b_i) \right) \\ &= \frac{\{(1-e)b_i k + e(1-b_i)k'\}d'_i + k}{d_i + 1} \end{aligned} \quad (16)$$

Similar to the Corollary 4.2, we can compare the separability of the two methods based on their coefficients.

**Corollary 4.5** (Discrimination power). *The difference of separation powers ( $Z$ ) between signed GCN and zero-weight GCN in multi-class graphs is given by:*

$$\begin{aligned} Z &= (1-2e)\{b_i k + (b_i - 1)k'\} - \{(1-e)b_i k + e(1-b_i)k'\} \\ &= -eb_i k + (1-e)(b_i - 1)k' \end{aligned} \quad (17)$$

Based on the above equation, we can induce the following conditional statement:

$$Z \in \begin{cases} (1-e-b_i)k, & \text{if } k' = -k \\ \{-2eb_i - (1-e-b_i)\}k, & \text{if } k' = k \end{cases} \quad (18)$$

Specifically, as the distribution of aggregated neighbors  $k'$  moves away from  $k$  (e.g.,  $k' = -k$ ),  $Z = 1 - e - b_i$  becomes identical to Eq. 10. This leads to the following equation,

$$\int_0^1 \int_0^1 (1-e-b_i) dedb_i = \left[ 1 - \frac{e^2 + b_i^2}{2} \right]_{e, b_i=0} = 0 \quad (19)$$

indicating that signed propagation outperforms the zero-weighting scheme. However, as  $k'$  gets closer to  $k$ , we claim that  $Z = -2eb_i + e + b_i - 1$  tends to be negative, where signed propagation may achieve dismal performance as below:

$$\begin{aligned} &\int_0^1 \int_0^1 (-2eb_i + e + b_i - 1) dedb_i \\ &= \left[ \frac{-eb_i^2 - e^2 b_i + e^2 + b_i^2}{2} - 1 \right]_{e, b_i=0} = -1 \end{aligned} \quad (20)$$

Intuitively, the probability of being  $\cos(k', k) = -1$  is inversely proportional to the number of entire classes. Thus, we can infer that zero-weight GCN generally outperforms signed one given multi-class datasets. As shown in Fig. 3, signed GCN outperforms zero-weight GCN only on the Pubmed

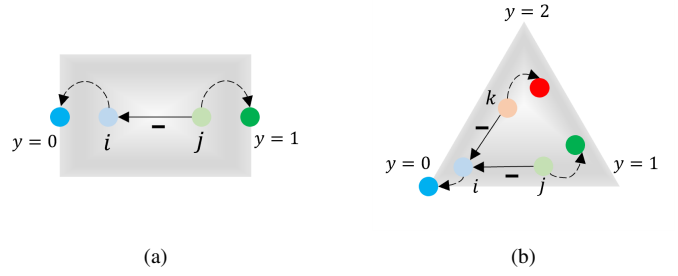


Fig. 4: Visualization of parameter update using the Dirichlet distribution (central side means higher prediction uncertainty). (a) Binary class case and (b) Multi-class case. In both cases, signed messages separate the ego and neighbors. However, in (b) multi-class case, the uncertainty of neighbors  $j$  and  $k$  increases

dataset which has the smallest number of classes (Table 3) among the datasets. Thus, we propose to manually adjust the messages from the neighbors ( $k'$ ) based on their similarity, denoted as edge weight calibration. The details are introduced in Section V-A, which guides  $k'$  to get closer to  $-k$  as in the upper case of Eq. 18 ( $Z = 1 - e - b_i$ ).

**Parameter update** (Signed propagation contributes to the ego-neighbor separation, but it also increases the prediction uncertainty under multiple class environments) Uncertainty management, which is closely related to the entropy [33], is vital in securing confident predictions [34, 35]. Here, we focus on the conflicting evidence [36, 37] which ramps up the entropy of outputs. One can easily measure the uncertainty of a prediction ( $\hat{y}_i$ ) using Shannon's entropy [38] as below:

$$H(\hat{y}_i) = - \sum_{j=1}^C \hat{y}_{i,j} \log_e \hat{y}_{i,j} \quad (21)$$

Now, we deduce a theorem regarding the uncertainty below.

**Theorem 4.6** (Uncertainty). *Signed messaging contributes to ego-neighbor separation (Eq. 13). However, as the training epoch  $t$  proceeds, the expectation of signed GNN prediction ( $\hat{y}_s$ ) exhibits higher uncertainty  $H(\mathbb{E}[\hat{y}_s])$  compared to that ( $\hat{y}_p$ ) of plain GNN  $H(\mathbb{E}[\hat{y}_p])$  as below:*

$$H(\mathbb{E}[\hat{y}_s^{(t+1)}]) - H(\mathbb{E}[\hat{y}_p^{(t+1)}]) > H(\mathbb{E}[\hat{y}_s^t]) - H(\mathbb{E}[\hat{y}_p^t]) \quad (22)$$

**Proof.** *Contrary to Eq. 13, we can infer that the true class probability ( $k$ ) of node  $p$  ( $\hat{y}_{p,k}$ ) increases, while other class probabilities  $\hat{y}_{p,o}$  ( $o \neq k$ ) decrease for plain GNN as follows:*

$$\hat{y}_p^{(t+1)} \in \begin{cases} \hat{y}_{p,k}^t - \eta \nabla_p \mathcal{L}_{\text{nil}}(Y_i, \hat{Y}_i)_k > \hat{y}_{p,k}^t \\ \hat{y}_{p,o}^t - \eta \nabla_p \mathcal{L}_{\text{nil}}(Y_i, \hat{Y}_i)_o < \hat{y}_{p,o}^t \quad \forall o \neq k \end{cases} \quad (23)$$

As shown in Eq. 13, the gradient of node  $s$  will have a reversed sign compared to node  $p$ . Thus, as the training epoch increases,  $\hat{y}_{p,k}$  will converge to 1 resulting in the decrease of  $H(\mathbb{E}[\hat{y}_p])$ . Conversely,  $\hat{y}_{s,k}$  gets closer to 0, which may fail to generate a highly confident prediction and lead to a surge of uncertainty. Thus, one can infer that  $H(\mathbb{E}[\hat{y}_s^{(t+1)}]) - H(\mathbb{E}[\hat{y}_p^{(t+1)}]) > H(\mathbb{E}[\hat{y}_s^t]) - H(\mathbb{E}[\hat{y}_p^t])$  as  $t \rightarrow \infty$ , which completes the proof.  $\square$

In Figure 4, we visualize the impact of signed propagation using the Dirichlet distribution. In both figures, signed messages contribute to the separation. However, in Fig 4b, the simultaneous increase in other class probabilities leads to the increment of conflict evidence. The solution to this will be introduced in § V-B as a confidence calibration.

## V. METHODOLOGY

We introduced the limitations of signed propagation in the multi-class scenario from two perspectives; message-passing and parameter update. Here, we propose two types of calibration, both of which belong to the self-training method [15, 39].

### A. (Message-Passing) Edge Weight Calibration

In Corollary 4.5, we analyze how signed propagation affects the distribution of neighbors ( $k'$ ). Particularly, we observe that the separability degrades when  $k'$  becomes similar to  $k$ . This observation suggests a mechanism to reduce the influence of heterogeneous neighbors. Thus, we propose the edge weight calibration based on the similarity of the two nodes, e.g., cosine similarity of  $l$ -th layer node features,  $\cos(h_i^l, h_j^l)$ . Then, we normalize the similarity score to make it belong to  $[0, 1]$ , followed by multiplying it with the original edge weight ( $A_{ij}$ ) as follows:

$$\forall (i, j) \in A, \tilde{A}_{ij} = \frac{\cos(h_i^l, h_j^l) + 1}{2} \cdot A_{ij} \quad (24)$$

One important thing is that we should also consider the sign of a message from multi-hop away nodes, which may be inconsistent through which information is transmitted. For example, we assume three nodes  $i, j, k$  that are connected serially and their edge weights are  $s_{ij}$  and  $s_{jk}$ , respectively. If  $y_i = y_j$ , then  $s_{ij} = 1$ , otherwise  $s_{ij} = -1$ . Under binary class, multi-hop edge weight  $s_{ij} \cdot s_{jk}$  is always consistent with the node label. However, under multiple classes, if the labels of three nodes are  $y_i = 0$ ,  $y_j = 1$ , and  $y_k = 2$ ,  $k$  is trained to be similar to  $i$  even though  $i$  and  $k$  are in different classes since  $s_{ij} \cdot s_{jk} = -1 \times -1 = 1$ . To address this, we modify the above equation using Jumping Knowledge [40], assuming  $l$ -hop message-passing as shown below:

$$\forall (i, j) \in \sum_{l=1}^L A^L, \tilde{A}_{ij} = \frac{\cos(h_i^l, h_j^l) + 1}{2} \cdot A_{ij} \quad (25)$$

Note that any type of  $A_{ij}$  (e.g., attention values) can be used for calibration. Below, we prove that edge weight calibration can enhance the separability of GNNs.

**Theorem 5.1** (Discrimination power after edge weight calibration). *Assuming that every class has the same population, the expectations of aggregated neighbors in signed GNN with and without the edge weight calibration are denoted as  $\mathbb{E}[|k'_{edge}|]$  and  $\mathbb{E}[|k'|]$ , respectively. Then, the two expectations comply with the following inequality relation.*

$$\mathbb{E}[|k'_{edge}|] = \frac{|k|}{d} \sqrt{\frac{c}{4} + \sum_{j=0}^c \cos\left(\frac{2\pi j}{c}\right)^2} > \mathbb{E}[|k'|] \quad (26)$$

In Eq. 17, we can substitute  $k'_{edge}$  into  $k$  and derive  $\mathbb{E}[Z] \leq \mathbb{E}[Z_{edge}]$  which demonstrates an increase in separability.

**Proof.** Similar to Eq. 15, we assume that  $|k'| \leq \mu$  and  $|k'_{edge}| \leq \mu$ . Since the discrimination power is determined based on the distance from the decision boundary, we can substitute  $k'$  and  $k'_{edge}$  in terms of  $k$ . Specifically, Eq. 17 can be redefined as below:

$$Z = -eb_i k + (1-e)(b_i - 1) \frac{\cos(k', k)|k'|}{|k'|} \\ Z_{edge} = -eb_i k + (1-e)(b_i - 1) \frac{\cos(k'_{edge}, k)|k'_{edge}|}{|k'_{edge}|} \quad (27)$$

Now, let's assume the number of classes is  $c$ , the average degree of nodes is  $d$ , and every class has the same population. Based on the above equation, one can compare the scale and direction between  $\cos(k', k)|k'|$  and  $\cos(k'_{edge}, k)|k'_{edge}|$  since other variables are the same. As  $k$  is a fixed vector (ego), the expectation of  $\cos(k', k)|k'|$  can be represented as,

$$\frac{|k|}{d} \sqrt{\left\{ \sum_{j=0}^c \cos\left(\frac{2\pi j}{c}\right) \right\}^2 + \left\{ \sum_{j=0}^c \sin\left(\frac{2\pi j}{c}\right) \right\}^2} \quad (28)$$

Under an identical class distribution, we can imagine an  $n$ -sided polygon inscribed in a circle, and the sum of the elements of the neighbor vectors  $k'$  is 0. By replacing  $c' = 2\pi/c$ , we can induce  $\cos(k'_{edge}, k)|k'_{edge}|$  as follows:

$$\mathbb{E}[\cos(k'_{edge}, k)|k'_{edge}|] \\ = \frac{|k|}{d} \sqrt{\left\{ \sum_{j=0}^c -\cos(jc') \right\}^2 + \left\{ \sum_{j=0}^c -\cos(jc') \sin(jc') \right\}^2} \\ = \frac{|k|}{d} \sqrt{\left\{ \sum_{j=0}^c \frac{-1 - \cos(2\pi jc')}{2} \right\}^2 + \left\{ \sum_{j=0}^c -\frac{\sin(2\pi jc')}{2} \right\}^2} \\ = \frac{|k|}{d} \sqrt{\frac{c}{4} + \sum_{j=0}^c \cos(jc')^2} > \mathbb{E}[\cos(k', k)|k'|] \quad (29)$$

Given that  $\mathbb{E}[\cos(k'_{edge}, k)|k'_{edge}|]$  has some positive value  $\alpha$ , we can infer the following inequality:

$$\mathbb{E}[Z_{edge}] = \mathbb{E}[Z] + \alpha > \mathbb{E}[Z] \quad (\alpha > 0) \quad (30)$$

which completes the proof.  $\square$

**Remark.** The edge weight calibration also enhances the quality of positive GNNs like GCN [2] and GAT [3] by reflecting the cosine similarity of two nodes [6] as below.

1) *Edge weight calibration for GCN:* We first explain how edge weight calibration improves the quality of positive GNNs. For brevity, we take the aggregation scheme of GCN [2]. Then, the expectation of node  $i$  after message-passing  $h_i^{(1)}$  becomes,

$$\mathbb{E}(h_i^{(1)} | v_i, d_i) = \frac{k}{d_i + 1} \\ + \sum_{j \in \mathcal{N}_i} \left( \frac{k(1-e) + ke}{d_{ij}} b_i + \frac{k'(1-e) + k'e}{d_{ij}} (1-b_i) \right) \\ = \frac{k}{d_i + 1} + \frac{\{kb_i + k'(1-b_i)\}d'}{d_i + 1} \quad (31)$$

Since the edge weight calibration multiplies the normalized cosine similarity  $0 \leq c \leq 1$ , the expectation of calibrated GCN can be redefined as follows:

$$\begin{aligned} \mathbb{E}(h_i^{(1)}|v_i, d_i) &= \frac{k}{d_i + 1} + \\ &\sum_{j \in \mathcal{N}_i} \left( \frac{k(1-e) + ke \times c}{d_{ij}} b_i + \frac{k'(1-e) \times c + k'e}{d_{ij}} (1-b_i) \right) \\ &= \frac{k}{d_i + 1} + \frac{\{(c-1)ke + k\}b_i + (1-c)k'e(1-b_i)}{d_i + 1} d' \end{aligned} \quad (32)$$

Using the above two equations, we can derive the discrimination power as below:

$$\begin{aligned} Z &= kb_i + k'(1-b_i) - \{(c-1)ke + k\}b_i - (1-c)k'e(1-b_i) \\ &= (1-c)keb_i + \{1 + (c-1)e\}k'(1-b_i) \end{aligned} \quad (33)$$

Given the above equation, we can induce the conditional statement as follows:

$$Z \in \begin{cases} e + b_i - 1 - ce & \text{if } \cos(k', k) = -1 \\ -(e + b_i - 1 - ce) - 2eb_i + 2eb_i c & \text{if } \cos(k', k) = 1, \end{cases} \quad (34)$$

Since  $\int_0^1 \int_0^1 (e + b_i - 1) dedb = \left[1 - \frac{e^2 + b^2}{2}\right]_{e,b=0}^1 = 0$ , we can induce that the first equation is smaller than 0. Furthermore, if we assume that  $c$  is sufficiently small  $c \rightarrow 0$ , the second equation becomes  $-2eb_i$ , which means that edge weight calibration improves the separability of positive GNNs.

2) *Edge weight calibration for GAT*: Since the attention value of GAT is always positive, we can induce a similar equation as above. Thus, instead of similar notational derivation, we show that the attention mechanism is not sufficient to capture the angular similarity of two nodes. Generally, the formulation of attention is defined as follows:

$$a_{ij} = \vec{a}^T [W\vec{h}_i || W\vec{h}_j] \quad (35)$$

The equation above implies that the attention weight is determined by the summation of distances between the attention vector  $\vec{a} = [\vec{a}_1 || \vec{a}_2]$  and two nodes  $W\vec{h}_i, W\vec{h}_j$  since  $a_{ij} = \vec{a}_1^T \cdot W\vec{h}_i + \vec{a}_2^T \cdot W\vec{h}_j$ . Now, let's assume that two neighbors,  $j$  and  $k$ , are equidistant from the attention vector. In such cases, the attention weight assigned to both  $j$  and  $k$  towards the ego node will be identical, regardless of their directional positioning. Consequently, attention may not effectively capture cosine similarity, where we show that edge weight calibration can enhance positive GNNs by incorporating angular information.

### B. (Parameter Update) Confidence Calibration

Theorem 4.6 shows that signed messages increase the uncertainty of predictions. To redeem this, we propose the calibration of predictions. This scheme boasts several advantages such as being free from path configuration, cost-efficient, and powerful. Here, we claim that various loss functions can be used for confidence calibration as below:

$$\mathcal{L}_{conf} \in \begin{cases} \frac{1}{N} \sum_{i=1}^N (-\max(\hat{y}_i) + \text{submax}(\hat{y}_i)) \\ \sum_{i=1}^N ||I - \hat{y}_i \hat{y}_i^T|| \end{cases} \quad (36)$$

---

### Algorithm 1 Pseudo-code: FAGCN [11] with our method

---

**Input:** Adjacency matrix ( $A$ ), initial node features ( $X$ ), node embedding at  $l^{th}$  layer ( $H^l$ ), attention weight between two nodes ( $a_{ij}$ ), initialized parameters of FAGCN ( $\theta$ ), edge weight threshold ( $\epsilon$ ), best validation score ( $\alpha^* = 0$ )

**Output:** Parameters with the best validation score ( $\theta^*$ )

- 1: **for** training epochs **do**
  - 2:   Retrieve  $l^{th}$  layer's node embedding,  $H^l$
  - 3:   Get node  $i$ 's embedding,  $h_i^l$
  - 4:   Get attention weights,  $a_{ij} = \text{tanh}(g^T [h_i^l || h_j^l])$
  - 5:   Normalize cosine similarity for edges in Eq. 25
  - 6:   Apply GNNs on  $\tilde{a}_{ij}$ ,  $\hat{Y} = \sigma(\bar{H}^{(L)})$
  - 7:   Compute node classification loss,  $\mathcal{L}_{EGNN}$
  - 8:   Compute calibration loss,  $\mathcal{L}_{conf}$
  - 9:   Get total loss,  $\mathcal{L}_{total} = \mathcal{L}_{EGNN} + \lambda \mathcal{L}_{conf}$
  - 10:   Update parameters,  $\theta' = \theta - \eta \frac{\partial \mathcal{L}_{total}}{\partial \theta}$
  - 11:   Using the updated parameters ( $\theta'$ ) and calibrated attention weights ( $a_{ij}$ ), get validation score  $\alpha$
  - 12:   **if**  $\alpha > \alpha^*$  **then**
  - 13:     Save current parameters,  $\theta^* = \theta'$
  - 14:     Update best validation score,  $\alpha^* = \alpha$
- 

The first one suppresses the maximal values and reduces the differences between the maximal and sub-maximal values, while the second one is a well-known orthogonal constraint. Both of them can be used to relieve the conflict evidence of predictions. Please note that any penalization strategy reducing entropy can be applied as a method of confidence calibration. One may argue that this is quite similar to the prior scheme [16, 41], but we provide a new understanding that signed propagation may incur higher uncertainty (Thm. 4.6).

### C. Optimization

During the training phase, we apply the edge (Eq. 25) and confidence calibration (Eq. 36) to reduce the uncertainty as,

$$\mathcal{L}_{total} = \mathcal{L}_{EGNN} + \lambda \mathcal{L}_{conf} \quad (37)$$

Here,  $\mathcal{L}_{EGNN}$  represents the node classification loss with the edge weight calibration, and  $\lambda$  is a hyper-parameter that adjusts the intensity of the confidence calibration. As in Figure 3, the enhanced performance of signed GCN (with calibration) substantiates the significant performance improvement attributable to our methodology. Additionally, note that this strategy is agnostic to specific GNN methodologies, which enables broad applicability across other frameworks [9–11] since it leverages only node similarity and predictions.

**(Reproducibility)** Our code is in anonymous *GitHub*<sup>1</sup>. Also, we introduce the pseudo-code of applying our method to one of the signed GNNs, FAGCN [11], in Algorithm 1.

## VI. EXPERIMENTS

We conduct extensive experiments to address the following research questions. We measure the node classification accu-

<sup>1</sup><https://anonymous.4open.science/tr/Signed-Calibrated-GNN-34B6/README.md>

TABLE I: (Q1) Node classification accuracy (%) with standard deviation on the six test datasets. **Bold** and underline indicates the 1<sup>st</sup> and 2<sup>nd</sup> best performances. Values in brackets represent the dissonance (Eq. 38) and methods with calibrations are marked with ‡.

Datasets $\mathcal{H}_g$ (Eq. 1)	Cora 0.81	Citeseer 0.74	Pubmed 0.8	Actor 0.22	Chameleon 0.23	Squirrel 0.22
GCN	79.0 ± 0.6 (0.17)	67.5 ± 0.8 (0.29)	77.6 ± 0.2 (0.53)	20.2 ± 0.4 (0.29)	49.3 ± 0.5 (0.19)	30.7 ± 0.7 (0.31)
<b>GCN</b> ‡	81.0 ± 0.9 (0.12)	71.3 ± 1.2 (0.14)	77.8 ± 0.4 (0.38)	21.7 ± 0.6 (0.62)	49.4 ± 0.6 (0.25)	31.5 ± 0.6 (0.58)
GAT	80.1 ± 0.6 (0.22)	68.0 ± 0.7 (0.25)	78.0 ± 0.4 (0.45)	22.5 ± 0.3 (0.28)	47.9 ± 0.8 (0.17)	30.8 ± 0.9 (0.27)
<b>GAT</b> ‡	81.4 ± 0.4 (0.12)	72.2 ± 0.6 (0.08)	78.3 ± 0.3 (0.39)	23.2 ± 1.8 (0.43)	49.2 ± 0.4 (0.16)	30.3 ± 0.8 (0.40)
GIN	77.3 ± 0.8 (0.33)	66.1 ± 0.6 (0.29)	77.1 ± 0.7 (0.47)	24.6 ± 0.8 (0.51)	49.1 ± 0.7 (0.26)	28.4 ± 2.2 (0.48)
APPNP	81.3 ± 0.5 (0.15)	68.9 ± 0.3 (0.21)	79.0 ± 0.3 (0.42)	23.8 ± 0.3 (0.49)	48.0 ± 0.7 (0.34)	30.4 ± 0.6 (0.69)
GCNII	81.1 ± 0.7 (0.08)	68.5 ± 1.4 (0.13)	78.5 ± 0.4 (0.20)	25.9 ± 1.2 (0.43)	48.1 ± 0.7 (0.21)	29.1 ± 0.9 (0.24)
H <sub>2</sub> GCN	80.6 ± 0.6 (0.16)	68.2 ± 0.7 (0.22)	78.5 ± 0.3 (0.29)	25.6 ± 1.0 (0.34)	47.3 ± 0.8 (0.19)	31.3 ± 0.7 (0.62)
ACM-GCN	80.2 ± 0.8 (0.24)	68.3 ± 1.1 (0.17)	78.1 ± 0.5 (0.31)	24.9 ± 2.0 (0.46)	49.5 ± 0.7 (0.20)	31.6 ± 0.4 (0.54)
HOG-GCN	79.7 ± 0.4 (0.31)	68.2 ± 0.6 (0.24)	78.0 ± 0.2 (0.29)	21.5 ± 0.5 (0.37)	47.7 ± 0.5 (0.32)	30.1 ± 0.4 (0.51)
JacobiConv	81.9 ± 0.6 (0.26)	69.6 ± 0.8 (0.19)	78.5 ± 0.4 (0.24)	25.7 ± 1.2 (0.30)	<b>52.8</b> ± 0.9 (0.21)	32.0 ± 0.6 (0.37)
GloGNN	82.4 ± 0.3 (0.33)	70.3 ± 0.5 (0.35)	79.3 ± 0.2 (0.26)	26.6 ± 0.7 (0.38)	48.2 ± 0.3 (0.27)	28.8 ± 0.8 (0.43)
PTDNet	81.2 ± 0.9 (0.24)	69.5 ± 1.2 (0.42)	78.8 ± 0.5 (0.44)	21.5 ± 0.6 (0.33)	50.6 ± 0.9 (0.17)	<u>32.1</u> ± 0.7 (0.34)
<b>PTDNet</b> ‡	81.9 ± 0.6 (0.20)	71.1 ± 0.8 (0.31)	79.0 ± 0.2 (0.38)	22.7 ± 0.6 (0.19)	50.9 ± 0.3 (0.15)	<b>32.3</b> ± 0.5 (0.30)
GPRGNN	82.2 ± 0.4 (0.25)	70.4 ± 0.8 (0.43)	79.1 ± 0.1 (0.26)	25.4 ± 0.5 (0.55)	49.1 ± 0.7 (0.25)	30.5 ± 0.6 (0.36)
<b>GPRGNN</b> ‡	<b>84.7</b> ± 0.2 (0.04)	<u>73.3</u> ± 0.5 (0.05)	<b>80.2</b> ± 0.2 (0.11)	<b>28.1</b> ± 1.3 (0.33)	<u>51.0</u> ± 0.4 (0.18)	31.8 ± 0.4 (0.16)
FAGCN	81.9 ± 0.5 (0.15)	70.8 ± 0.6 (0.17)	79.0 ± 0.5 (0.31)	25.2 ± 0.8 (0.66)	46.5 ± 1.1 (0.25)	30.4 ± 0.4 (0.64)
<b>FAGCN</b> ‡	<u>84.1</u> ± 0.4 (0.09)	<b>73.8</b> ± 0.5 (0.08)	<u>79.7</u> ± 0.2 (0.16)	<u>27.6</u> ± 0.5 (0.42)	48.8 ± 0.7 (0.13)	31.3 ± 0.5 (0.37)
GGCN	81.0 ± 1.2 (0.38)	70.7 ± 1.6 (0.30)	78.2 ± 0.4 (0.47)	22.5 ± 0.5 (0.47)	48.5 ± 0.7 (0.15)	30.2 ± 0.7 (0.40)
<b>GGCN</b> ‡	83.9 ± 0.8 (0.07)	73.0 ± 0.4 (0.05)	78.9 ± 0.3 (0.29)	24.6 ± 0.4 (0.26)	50.0 ± 0.4 (0.07)	31.1 ± 0.6 (0.15)

TABLE II: Statistical details of the six benchmark datasets

Datasets	Cora	Citeseer	Pubmed	Actor	Cham.	Squirrel
# Nodes	2,708	3,327	19,717	7,600	2,277	5,201
# Edges	10,558	9,104	88,648	25,944	33,824	211,872
# Features	1,433	3,703	500	931	2,325	2,089
# Labels	7	6	3	5	5	5

rary of all methods following the settings in [2], where the parameters are optimized solely with the training nodes.

- **Q1** Do the proposed methods improve the node classification accuracy of graph neural networks?
- **Q2** Do the signed messages cause an increase in the uncertainty of the final prediction?
- **Q3** How much impact do the two calibration methodologies have on performance improvement?
- **Q4** How does the weight of the confidence calibration, denoted as  $\lambda$  (Eq. 37) affect the overall performance?

**Baselines.** We employ several state-of-the-art methods for validation and comparison: (1) GNNs with positive edge weights: GCN [2], GAT [3], GIN [42], APPNP [43], GCNII [44], H<sub>2</sub>GCN [4], ACM-GCN [45], HOG-GCN [25], JacobiConv [46], and GloGNN [8]. (2) Edge pruning GNN: PTDNet [13]. (3) GNNs with signed propagation: GPRGNN [10], FAGCN [11], and GGCN [9].

### A. Experimental Results (Q1)

In Table I, we describe the node classification accuracy of each method. We also show dissonance within parentheses. Dissonance is an uncertainty metric, a measure of effectiveness in distinguishing out-of-distribution data from conflict predic-

tions [37, 47]:

$$diss(\hat{y}_i) = \sum_{j=1}^C \left( \frac{\hat{y}_{ij} \sum_{k \neq j} \hat{y}_{ik} (1 - \frac{|\hat{y}_{ik} - \hat{y}_{ij}|}{\hat{y}_{ij} + \hat{y}_{ik}})}{\sum_{k \neq j} \hat{y}_{ik}} \right) \quad (38)$$

The above equation can be computed for the non-zero values of  $\hat{y}_i$ . The performance in Table I is inferior to the benchmarks since we chose the test scores with the best validation.

**Homophily ratio plays an important role in GNNs.** On the three homophilic citation networks, we observe that all methods perform well. As the homophily ratio decreases, methods that adjust weights based on associativity start to outperform plain GNNs. Similarly, methods of using signed messages (GPRGNN, FAGCN, and GGCN) or separating ego and neighbors (H<sub>2</sub>GCN) are shown to be effective in our experiments. However, for the two highly heterophilic graphs (Chameleon and Squirrel), where many nodes share the same neighborhoods [48], we notice that blocking information (PTDNet) outperforms signed GNNs.

**Calibrations are effective in improving accuracy as well as in alleviating uncertainty.** We apply calibrations (‡) to three state-of-the-art methods that employ signed propagation (GPRGNN, FAGCN, and GGCN). The average improvements achieved by applying calibrations to these three methods are 4.37%, 3.1%, and 3.13%, respectively. Although calibrations help to improve the performances of plain GCN‡ (2.65%), GAT‡ (1.97%), and PTDNet‡ (1.68%), it is shown to be more effective for signed messaging. In addition to this, we can also observe that the calibrated methods show lower dissonance (Eq. 38) compared to the corresponding vanilla model. To summarize, the results indicate that calibration not only reduces uncertainty but also improves accuracy significantly.



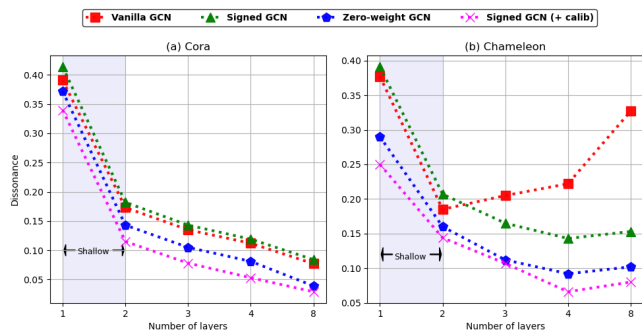


Fig. 5: (Q2) Dissonance of vanilla GCN and its two variants; signed and zero-weight, which is the same as the one in Figure 3. The left one is Cora and the right one is the Chameleon dataset

### B. Signed Propagation and Uncertainty (Q2)

To demonstrate the effect of signed messaging on uncertainty, we measure the dissonance using two variants of GCN; one variant assigns -1 and the other assigns zeros to heterophilic edges, respectively (please refer to §IV-C for details). The results are presented in Fig. 5 where the x-axis is the number of layers and the y-axis represents dissonance. Here, we conducted experiments with the Cora (Fig. 4a) and Chameleon (Fig. 4b) datasets. As stated in Thm. 4.6, the signed GCN variant in the green-colored line exhibits higher uncertainty compared to the zero-weight variant. In the Chameleon dataset, the entropy of vanilla GCN increases as the layer gets deeper, indicating that positive message-passing fails to deal adequately with heterophily. Although zero-weight GCN shows lower dissonance, signed GCN with calibrations consistently produces the smallest uncertainty, highlighting the efficacy of our method in mitigating such limitations.

TABLE III: (Q3) Ablation study. We describe the node classification accuracy with standard deviation by applying either the edge weight calibration or the confidence calibration to signed GNNs

Datasets	Cora	Citeseer	Actor	Chameleon
GPRGNN	82.2 $\pm$ 0.4	70.4 $\pm$ 0.8	25.4 $\pm$ 0.5	49.1 $\pm$ 0.9
+ edge calib	83.3 $\pm$ 0.6	71.5 $\pm$ 1.0	26.3 $\pm$ 0.6	49.7 $\pm$ 0.7
+ conf calib	<b>83.8</b> $\pm$ 0.5	72.6 $\pm$ 0.5	<b>27.5</b> $\pm$ 0.4	<b>50.2</b> $\pm$ 0.3
FAGCN	81.9 $\pm$ 0.5	70.8 $\pm$ 0.6	25.2 $\pm$ 0.8	46.5 $\pm$ 1.1
+ edge calib	82.8 $\pm$ 0.6	72.3 $\pm$ 0.7	25.8 $\pm$ 0.7	46.9 $\pm$ 1.0
+ conf calib	83.5 $\pm$ 0.3	<b>73.4</b> $\pm$ 0.5	26.3 $\pm$ 0.4	48.0 $\pm$ 0.8
GGCN	81.0 $\pm$ 1.2	70.7 $\pm$ 1.6	22.5 $\pm$ 0.5	48.5 $\pm$ 0.7
+ edge calib	82.9 $\pm$ 1.0	71.0 $\pm$ 1.1	23.3 $\pm$ 0.6	48.9 $\pm$ 0.7
+ conf calib	83.7 $\pm$ 0.9	72.5 $\pm$ 0.6	23.6 $\pm$ 0.4	49.6 $\pm$ 0.5

### C. Ablation Study (Q3)

We conduct an ablation study to test the relative effectiveness of the two calibration methods. In Table III, we describe the node classification accuracy of signed GNNs on the homophilic (Cora, Citeseer) and heterophilic (Actor, Chameleon) graphs. Here, we apply either the edge weight calibration (+ edge calib) or the confidence calibration (+ conf calib). From the table, we can see that the methods equipped with the confidence calibration generally outperform

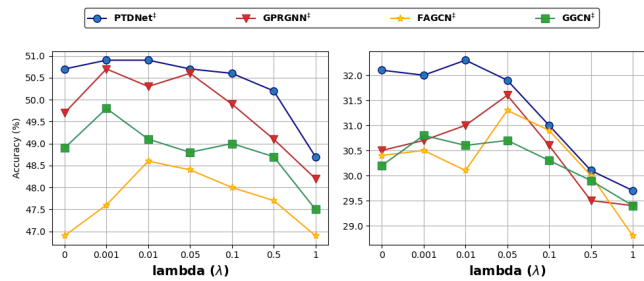


Fig. 6: (Q4) Node classification accuracy w.r.t. the parameter  $\lambda$  which controls the weight of the confidence calibration. Each figure represents a Chameleon (left) and Squirrel (right)

the edge weight calibration and exhibit smaller variances. This is because the confidence calibration reduces the uncertainty of all nodes during training while the edge calibration is only applied to a (small) subset of edges during testing. Also, edge calibration is beneficial, preventing the propagation of signed information from similar nodes.

### D. Parameter Sensitivity Analysis (Q4)

We conduct experiments to investigate the effect of the confidence calibration by adjusting  $\lambda$  (Eq. 37). In Figure 6, we varied the values of  $\lambda$  from 0 to 1. The edge weight calibration is combined with all methods along with the confidence calibration. The blue line represents PTDNet, while the others are signed GNNs. Notably, in both figures, calibrations improve the quality of all methods and are shown to be more effective in signed GNNs than in PTDNet, particularly in terms of relieving uncertainty. Also, finding an appropriate lambda is beneficial for overall improvement since assigning higher values to  $\lambda$  generally degrades the overall performance, necessitating the use of early stopping during training. Additionally, please note that calibration can be limited by the inherent low capability of base models in heterophilic graphs, where it acts as a downstream task of GNNs.

## VII. CONCLUSION

We present new theoretical insights on the effect of using signed messages in multi-class graphs. In contrast to previous theorems that assume graphs with binary classes and solely focus on message-passing, we extend them to multi-class scenarios and introduce a new perspective on parameter updates. From this viewpoint, we highlight two critical limitations of using signed propagation: (1) It suffers from reduced separability in multi-class graphs with high possibility, and (2) It increases the probability of generating conflicting evidence compared to positive message-passing schemes. Based on these observations, we propose the edge weight and confidence calibrations as solutions to enhance performance and alleviate uncertainty. Our extensive performance experiments on six real-world datasets show that the calibration techniques are effective for both signed and plain GNNs. We believe that our theorems offer valuable insights for the development of improved aggregation schemes in future studies.

## REFERENCES

- [1] M. Defferrard, X. Bresson, and P. Vandergheynst, "Convolutional neural networks on graphs with fast localized spectral filtering," *Advances in neural information processing systems*, vol. 29, 2016.
- [2] T. N. Kipf and M. Welling, "Semi-supervised classification with graph convolutional networks," *arXiv preprint arXiv:1609.02907*, 2016.
- [3] P. Velickovic, G. Cucurull, A. Casanova, A. Romero, P. Lio, and Y. Bengio, "Graph attention networks," *stat*, vol. 1050, p. 20, 2017.
- [4] J. Zhu, Y. Yan, L. Zhao, M. Heimann, L. Akoglu, and D. Koutra, "Beyond homophily in graph neural networks: Current limitations and effective designs," *Advances in Neural Information Processing Systems*, vol. 33, pp. 7793–7804, 2020.
- [5] Y. Ma, X. Liu, N. Shah, and J. Tang, "Is homophily a necessity for graph neural networks?" *arXiv preprint arXiv:2106.06134*, 2021.
- [6] S. Brody, U. Alon, and E. Yahav, "How attentive are graph attention networks?" *arXiv preprint arXiv:2105.14491*, 2021.
- [7] H. Pei, B. Wei, K. C.-C. Chang, Y. Lei, and B. Yang, "Geom-gcn: Geometric graph convolutional networks," *arXiv preprint arXiv:2002.05287*, 2020.
- [8] X. Li, R. Zhu, Y. Cheng, C. Shan, S. Luo, D. Li, and W. Qian, "Finding global homophily in graph neural networks when meeting heterophily," *arXiv preprint arXiv:2205.07308*, 2022.
- [9] Y. Yan, M. Hashemi, K. Swersky, Y. Yang, and D. Koutra, "Two sides of the same coin: Heterophily and oversmoothing in graph convolutional neural networks," *arXiv preprint arXiv:2102.06462*, 2021.
- [10] E. Chien, J. Peng, P. Li, and O. Milenkovic, "Adaptive universal generalized pagerank graph neural network," *arXiv preprint arXiv:2006.07988*, 2020.
- [11] D. Bo, X. Wang, C. Shi, and H. Shen, "Beyond low-frequency information in graph convolutional networks," *arXiv preprint arXiv:2101.00797*, 2021.
- [12] F. Di Giovanni, J. Rowbottom, B. P. Chamberlain, T. Markovich, and M. M. Bronstein, "Graph neural networks as gradient flows," *arXiv preprint arXiv:2206.10991*, 2022.
- [13] D. Luo, W. Cheng, W. Yu, B. Zong, J. Ni, H. Chen, and X. Zhang, "Learning to drop: Robust graph neural network via topological denoising," in *Proceedings of the 14th ACM International Conference on Web Search and Data Mining*, 2021, pp. 779–787.
- [14] B. Aseem, F. Kimon, J. Aukosh, and a. et, "Effects of graph convolutions in multi-layer networks," in *The Eleventh International Conference on Learning Representations*, 2023.
- [15] C. Guo, G. Pleiss, Y. Sun, and K. Q. Weinberger, "On calibration of modern neural networks," in *International conference on machine learning*. PMLR, 2017, pp. 1321–1330.
- [16] X. Wang, H. Liu, C. Shi, and C. Yang, "Be confident! towards trustworthy graph neural networks via confidence calibration," *Advances in Neural Information Processing Systems*, vol. 34, pp. 23 768–23 779, 2021.
- [17] M. Morris, B. C. Grau, and I. Horrocks, "Orbit-equivariant graph neural networks," in *The Twelfth International Conference on Learning Representations*, 2023.
- [18] F. Barbero, A. Velingker, A. Saberi, M. Bronstein, and F. Di Giovanni, "Locality-aware graph-rewiring in gnns," *arXiv preprint arXiv:2310.01668*, 2023.
- [19] Y. Choi, J. Choi, T. Ko, H. Byun, and C.-K. Kim, "Finding heterophilic neighbors via confidence-based subgraph matching for semi-supervised node classification," in *Proceedings of the 31st ACM International Conference on Information & Knowledge Management*, 2022, pp. 283–292.
- [20] K. Zhao, Q. Kang, Y. Song, R. She, S. Wang, and W. P. Tay, "Graph neural convection-diffusion with heterophily," *arXiv preprint arXiv:2305.16780*, 2023.
- [21] S. Chanpuriya and C. Musco, "Simplified graph convolution with heterophily," *arXiv preprint arXiv:2202.04139*, 2022.
- [22] J. Choi, S. Hong, N. Park, and S.-B. Cho, "Gread: Graph neural reaction-diffusion networks," in *International Conference on Machine Learning*. PMLR, 2023, pp. 5722–5747.
- [23] Y. Sun, H. Deng, Y. Yang, C. Wang, J. Xu, R. Huang, L. Cao, Y. Wang, and L. Chen, "Beyond homophily: Structure-aware path aggregation graph neural network," in *Proceedings of the Thirty-First International Joint Conference on Artificial Intelligence, IJCAI-22*, L. D. Raedt, Ed. International Joint Conferences on Artificial Intelligence Organization, 7 2022, pp. 2233–2240, main Track. [Online]. Available: <https://doi.org/10.24963/ijcai.2022/310>
- [24] J. Zhu, R. A. Rossi, A. Rao, T. Mai, N. Lipka, N. K. Ahmed, and D. Koutra, "Graph neural networks with heterophily," in *Proceedings of the AAAI Conference on Artificial Intelligence*, vol. 35, 2021.
- [25] T. Wang, D. Jin, R. Wang, D. He, and Y. Huang, "Powerful graph convolutional networks with adaptive propagation mechanism for homophily and heterophily," in *Proceedings of the AAAI Conference on Artificial Intelligence*, vol. 36, 2022, pp. 4210–4218.
- [26] X. Zheng, M. Zhang, C. Chen, Q. Zhang, C. Zhou, and S. Pan, "Autoheg: Automated graph neural network on heterophilic graphs," *arXiv preprint arXiv:2302.12357*, 2023.
- [27] Z. Fang, L. Xu, G. Song, Q. Long, and Y. Zhang, "Polarized graph neural networks," in *Proceedings of the ACM Web Conference 2022*, 2022, pp. 1404–1413.
- [28] Y. Guo and Z. Wei, "Clenshaw graph neural networks," *arXiv preprint arXiv:2210.16508*, 2022.
- [29] A. Baranwal, K. Fountoulakis, and A. Jagannath, "Graph convolution for semi-supervised classification: Improved linear separability and out-of-distribution generalization," *arXiv preprint arXiv:2102.06966*, 2021.
- [30] H. Ni and T. Maehara, "Revisiting graph neural networks: All we have is low-pass filters," *arXiv preprint arXiv:1905.09550*, 2019.
- [31] K. Oono and T. Suzuki, "Graph neural networks exponentially lose expressive power for node classification," *arXiv preprint arXiv:1905.10947*, 2019.
- [32] Z. Chen, T. Ma, and Y. Wang, "When does a spectral graph neural network fail in node classification?" *arXiv preprint arXiv:2202.07902*, 2022.
- [33] H. Liu, B. Hu, X. Wang, C. Shi, Z. Zhang, and J. Zhou, "Confidence may cheat: Self-training on graph neural networks under distribution shift," in *Proceedings of the ACM Web Conference 2022*, 2022, pp. 1248–1258.
- [34] J. Moon, J. Kim, Y. Shin, and S. Hwang, "Confidence-aware learning for deep neural networks," in *international conference on machine learning*. PMLR, 2020, pp. 7034–7044.
- [35] S. Mukherjee and A. Awadallah, "Uncertainty-aware self-training for few-shot text classification," *Advances in Neural Information Processing Systems*, vol. 33, pp. 21 199–21 212, 2020.
- [36] C. Perry, "Machine learning and conflict prediction: a use case," *Stability: International Journal of Security and Development*, vol. 2, no. 3, p. 56, 2013.
- [37] X. Zhao, F. Chen, S. Hu, and J.-H. Cho, "Uncertainty aware semi-supervised learning on graph data," *Advances in Neural Information Processing Systems*, vol. 33, pp. 12 827–12 836, 2020.
- [38] C. E. Shannon, "A mathematical theory of communication," *The Bell system technical journal*, vol. 27, no. 3, pp. 379–423, 1948.
- [39] H. Yang, K. Ma, and J. Cheng, "Rethinking graph regularization for graph neural networks," in *Proceedings of the AAAI Conference on Artificial Intelligence*, vol. 35, 2021, pp. 4573–4581.
- [40] K. Xu, C. Li, Y. Tian, T. Sonobe, K.-i. Kawarabayashi, and S. Jegelka, "Representation learning on graphs with jumping knowledge networks," in *International conference on machine learning*. PMLR, 2018.
- [41] K. Guo, K. Zhou, X. Hu, Y. Li, Y. Chang, and X. Wang, "Orthogonal graph neural networks," in *Proceedings of the AAAI Conference on Artificial Intelligence*, vol. 36, 2022, pp. 3996–4004.
- [42] K. Xu, W. Hu, J. Leskovec, and S. Jegelka, "How powerful are graph neural networks?" *arXiv preprint arXiv:1810.00826*, 2018.
- [43] J. Klicpera, A. Bojchevski, and S. Günnemann, "Predict then propagate: Graph neural networks meet personalized pagerank," *arXiv preprint arXiv:1810.05997*, 2018.
- [44] M. Chen, Z. Wei, Z. Huang, B. Ding, and Y. Li, "Simple and deep graph convolutional networks," in *International Conference on Machine Learning*. PMLR, 2020, pp. 1725–1735.
- [45] S. Luan, C. Hua, Q. Lu, J. Zhu, M. Zhao, S. Zhang, X.-W. Chang, and D. Precup, "Revisiting heterophily for graph neural networks," *arXiv preprint arXiv:2210.07606*, 2022.
- [46] X. Wang and M. Zhang, "How powerful are spectral graph neural networks," in *International Conference on Machine Learning*. PMLR, 2022, pp. 23 341–23 362.
- [47] T. Huang, D. Wang, and Y. Fang, "End-to-end open-set semi-supervised node classification with out-of-distribution detection," in *Proceedings of the Thirty-First International Joint Conference on Artificial Intelligence, IJCAI-22*. IJCAI, 2022.
- [48] O. Platonov, D. Kuznedelev, M. Diskin, A. Babenko, and L. Prokhorenkova, "A critical look at the evaluation of gnns under heterophily: are we really making progress?" *arXiv preprint arXiv:2302.11640*, 2023.